Available online at www.sciencedirect.com
ScienceDirect
Journal of the European Ceramic Society 27 (2007) 1487–1491
www.elsevier.com/locate/jeurceramsoc

Study of the amplitude-dependent mechanical behaviour of yttria-stabilised zirconia thermal barrier coatings

N. Tassini [a,*], K. Lambrinou [b], I. Mircea [c], M. Bartsch [c], S. Patsias [a], O. Van der Biest [b]

[a] *Dynamics Research Group, Department of Mechanical Engineering, University of Sheffield, Mappin Street, Sheffield S1 3JD, United Kingdom*
[b] *Department of Metallurgy and Materials Engineering, Katholieke Universiteit Leuven, Kasteelpark Arenberg 44, B-3001 Heverlee, Belgium*
[c] *Institute of Materials Research, German Aerospace Center (DLR), Linder Höhe, D-51147 Köln, Germany*

Available online 12 June 2006

Abstract

Widely used in turbines for propulsion and power generation, thermal barrier coatings (TBCs) increase the efficiency of turbine engines by allowing them to work at higher temperatures, due to their thermal insulating properties. Typically TBC systems consist of a metallic bondcoat (BC) and a ceramic topcoat (TC). Previous research has revealed that ceramic TCs possess an amplitude-dependent mechanical behaviour and that they can be used as damping treatments, due to their good damping properties. The microstructure and the properties of ceramic TCs vary significantly depending on the employed deposition technique. This work investigates the differences in the mechanical behaviour of yttria-stabilised zirconia (YSZ with 8 wt% yttria) TC deposited by atmospheric plasma spraying (APS) and electron beam-physical vapour deposition (EB-PVD), by means of tests run with the amplitude dependent damping (ADD) test rig and of scanning electron microscopy (SEM) analysis.

Keywords: Mechanical properties; Non-destructive evaluation; ZrO_2; Microstructure-final; Amplitude-dependence

1. Introduction

Thermal barrier coatings (TBCs) are used in a wide range of applications for their thermal insulation properties,[1] with propulsion and power generation turbines being the most interesting ones. TBCs reduce the substrate's temperature by means of their structure: the systems are usually constituted of two layers, a metallic bondcoat (BC) to protect the substrate against oxidation and a ceramic topcoat (TC), which actually possesses the thermal insulating properties. The materials used for the ceramic layer are mainly oxide ceramics, since they possess low thermal conductivities, with 8 wt% yttria stabilised zirconia (8YSZ) being the most widely used because it provides the best performance in high temperature applications.[2] Ceramic coatings can be applied using various deposition techniques, which may be divided based on their working principle. Different coating deposition techniques generate very different microstructures, although the initial ceramic material might be the same; this results in different mechanical properties of the different coatings.[3] The two major deposition techniques are plasma spraying (PS) and electron beam-physical vapour deposition (EB-PVD). Recent studies have shown that ceramic coatings provide sufficient levels of damping to be a valid alternative to traditional damping treatments.[4–6] Moreover, these properties are virtually unaltered up to temperatures of 600 °C. Since the very first work that introduced the damping properties of ceramic coatings,[7] it has been shown that PS ceramic coatings possess an amplitude-dependent damping and stiffness behaviour. The level of damping and the resonance frequency of coated specimens vary with the vibration strain they undergo.

The elastic properties of PS ceramic coating have been studied in various works. Kroupa and Plesek[8] have linked these properties to the microstructural defects. This has been possible by reducing the complexity of the porous spaces to four families of defects, as shown in Fig. 1: larger irregular voids between the splats of ceramic, small spherical pores inside the splats, "intersplat" cracks between the splats and "intrasplat" microcracks within the splats directed perpendicularly the plane of the splats. The small elastic openings and partial closing of the intersplat and intrasplats cracks are considered to be the responsible for the elastic behaviour of PS ceramic coatings. Patsias and Williams[5] described other non-linear features of ceramic coatings, over the above mentioned amplitude dependence. The mechanical

* Corresponding author. Tel.: +44 114 222 7870; fax: +44 114 222 7890.
E-mail address: n.tassini@sheffield.ac.uk (N. Tassini).

0955-2219/$ – see front matter © 2006 Elsevier Ltd. All rights reserved.
doi:10.1016/j.jeurceramsoc.2006.05.041

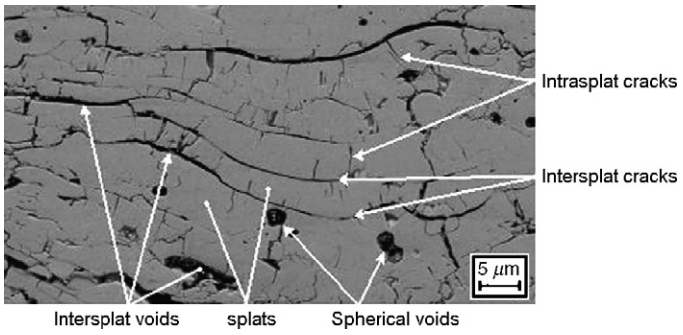

Fig. 1. SEM micrograph showing a cross-section through the microstructure of an APS-deposited 8YSZ coating.

properties have been shown to be affected by long-term (or permanent) effects and short-term (or "memory") effects.

2. Experimental procedure

2.1. Materials characterisation technique

Specimens coated with different coatings types have been tested at the University of Sheffield in order to elucidate the following aspects of their non-linear mechanical behaviour: (a) strain amplitude dependence, (b) dependence of the mechanical properties on the microstructure and the deposition technique and (c) strain history dependence.

The non-linear mechanical behaviour of ceramic coatings requires a special characterisation procedure, since standard techniques cannot be used. In the past few years a mixed experimental–numerical procedure has been developed at the University of Sheffield for the characterisation of the non-linear properties of ceramic coatings. This procedure is built around a custom-built test-rig, the amplitude dependent damping (ADD) test rig,[4] and is capable of running tests over a wide range of strain amplitudes.

In the ADD test rig, a specimen covered with a ceramic coating is clamped at one end and is free to vibrate at the other end, while it is excited through the base. Once the excitation force is removed the amplitude of vibration decays at a certain rate and frequency. Through a numerical analysis the damping ratios[9] and the resonant frequencies of the coated beam are obtained from the decay.[4] These results are subsequently used in an inverse finite element (FE) routine to estimate the Young's modulus and loss factor of the ceramic material of the coating.[3] This is possible by implementing an exact FE model of the coated beam with a variable Young's modulus for the ceramic coating material. The model is run iteratively with the same boundary conditions of the tests, that is one end is clamped and one end is free to vibrate (i.e. clamped-free); once the resulting frequency of the beam matches the experimental results, the Young's modulus is accepted. The loss factor of the coating's material is calculated subsequently with a procedure based on the modal strain energy (MSE) method.[10] This procedure is repeated for every set of experimental results at different strain levels.

Table 1
List of specimens tested

Reference no.	Coating	Coating thickness (mm)
S1N25	Uncoated	–
S1N11	APS 8YSZ	0.32
S1N14	APS BC and EB-PVD 8YSZ	0.04, 0.28
S1N19	APS BC and APS 8YSZ	0.07, 0.37

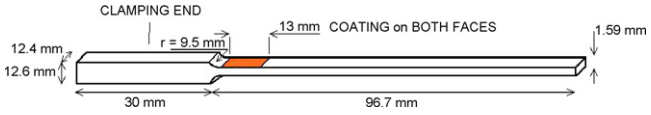

Fig. 2. Geometry of specimen tested with ADD test rig at the University of Sheffield (S1N11, S1N14 and S1N19).

2.2. Description of tested materials

The mixed experimental–numerical procedure has been used to test specimens coated by APS and EB-PVD techniques. The specimens used for this work are listed in Table 1 together with their coatings configurations. The geometry of specimens tested at the University of Sheffield is shown in Fig. 2. The position and coverage of the coating's layers in the coated specimens correspond to the areas of uniform strain for the first flexural mode (maximum variation of 12.4%), which has been used throughout all the tests with the ADD test rig. This is to take into account the strain amplitude dependence of ceramic coatings, and relate their mechanical properties to the strain amplitude at the interface substrate and coating. All the specimens were manufactured with Inconel® 625 super alloy (In625), a nickel–chromium–molybdenum alloy with low damping to reduce interference with the damping properties of the ceramic coatings. In this work the BC material was APS deposited NiCoCrAlY and was applied only on the EB-PVD ceramic-coated specimen (S1N14) since the protection of the substrate from oxidation is optional when APS TCs are applied but becomes necessary for EB-PVD ones because of the higher temperatures involved during the deposition procedure. The material selected for the ceramic coating is 8 wt% yttria-stabilised zirconia, commonly used for TBCs.[2] The properties of the materials used are given in Table 2. The values for In625 properties were obtained during previous tests on an uncoated specimen in K.U. Leuven, while the properties of the BC were obtained from Ref.[11] The density of the 8YSZ coating was obtained by measuring mass and volume of a sample while the Poisson ratio's value was taken from Ref.[12] A FE model was created for each specimen using 20-node quadratic brick elements, reduced integration (C3D20R)

Table 2
Properties of materials used

Material	E (GPa)	ν	ρ (kg/m^3)
In625	201.67	0.307	8370
APS BC (NiCoCrAlY)	137.9	0.27	7800
APS 8YSZ	–	0.3	4080
EB-PVD 8YSZ	–	0.3	4780

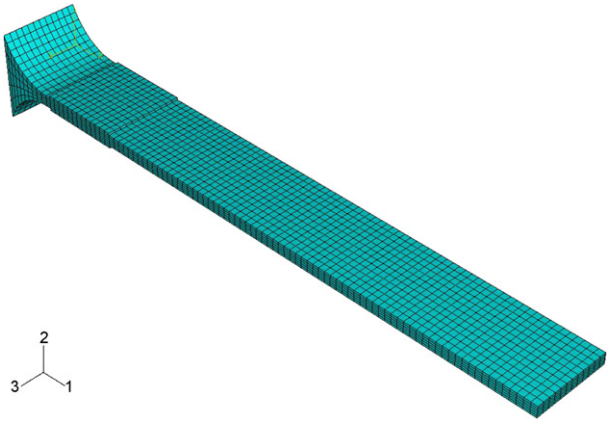

Fig. 3. FE model of specimen S1N11.

with ABAQUS 6.3[13]; the model for specimens S1N11 is shown in Fig. 3.

3. Results and discussion

The analysis was first applied on experimental results obtained on specimen S1N11 and S1N14, to compare the Young's moduli and loss factor for EB-PVD 8YSZ coating against APS 8YSZ: the results are plotted in Fig. 4a and b. As it is clear from the two plots, both stiffness and damping of the two coatings are amplitude dependant, with the APS coating demonstrating stronger dependence on amplitude. Fig. 4a shows that the EB-PVD coating provides up to 77% higher Young's modulus than the APS coating, while from Fig. 4b it is clear that the APS possesses higher damping (up to five times). The differences can be explained by considering their two very different microstructures as results from the SEM analysis done by K.U. Leuven: the two structures are compared in Fig. 5. The lower Young's modulus of the APS coating can be due to the "freedom" of the microsplats to move along the flexural direction; these movements are minimal in the EB-PVD structure because under flexure the ceramic columns on the compression side are in contact, which accounts for their higher stiffness. Following the results of Kroupa mentioned in Section 2,[8] the authors believe that the damping in APS coating arises from the sliding of the surfaces along the defects present in their microstructure. The nature of the load applied to the specimens tested for this work, maximise the sliding along these surfaces. This explanation is also supported by the fact that since the very first work on the damping properties of PS coatings,[7] the nature of their damping was considered to be friction between internal surfaces, as shown experimentally in Ref.[14] In EB-PVD coatings the relative sliding between columns due to flexural tests is limited, resulting in lower energies dissipated by friction and thus in lower damping than APS coatings. Specimen S1N19 was tested at different starting strain levels during 5 days of tests following the order given in Table 3. The test plan was designed to establish the strain history dependence of the mechanical properties of ceramic coatings. Fig. 6 shows the results for the added damping (Q^{-1} factor) due to the coating: the five curves of damping

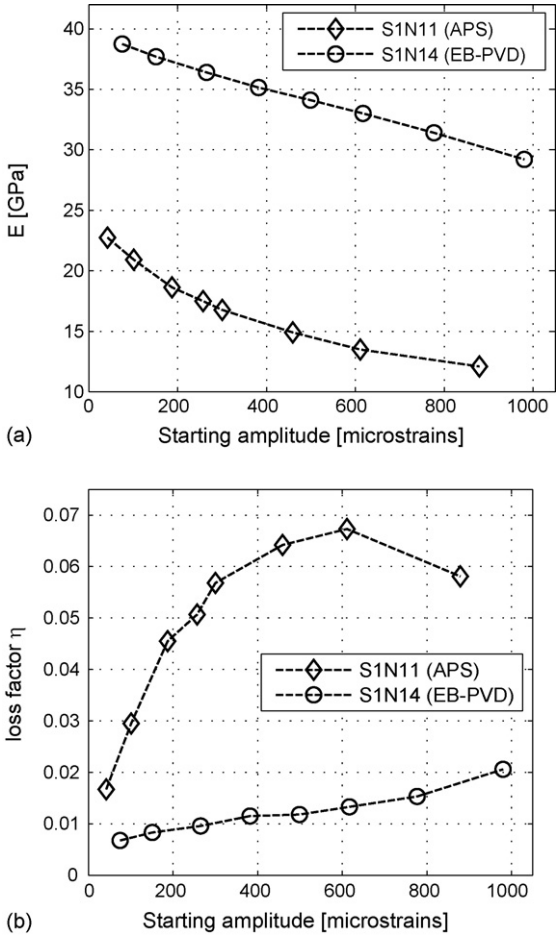

Fig. 4. (a) Young's modulus and (b) loss factor of APS and EB-PVD 8YSZ coatings as found with the ADD test rig and FE analysis on specimens S1N11 and S1N14.

are obtained from decays after the beam has been excited at the first strain level of each day of testing. These curves have been obtained by subtracting from the damping of the coated beam, the damping of the uncoated reference beam (S1N26), shown with a solid line in Fig. 6. The curves show that the damping depends on the strain history of the ceramic-coated beam, in particular the damping increases as the beam is subjected to session of vibrations. This result can be related to a work carried out by Van Den Abeele[15] concerning the damping of reinforced concrete beams, where it was found that increasing levels of vibration in the beams caused an accumulation of internal damage in the form of microcracks, which was reflected in an increase of its damping. The microstructure of the damaged reinforced concrete is very similar to that of APS coatings,

Table 3
Order of strain levels applied to specimen S1N19

Day of test	Starting strain levels tested ($\mu\varepsilon$)
1st	170
2nd	150–260–150
3rd	150–260–500–260–150
4th	150–260–500–850–500–260–150
5th	150–260–500–850–500–260–150

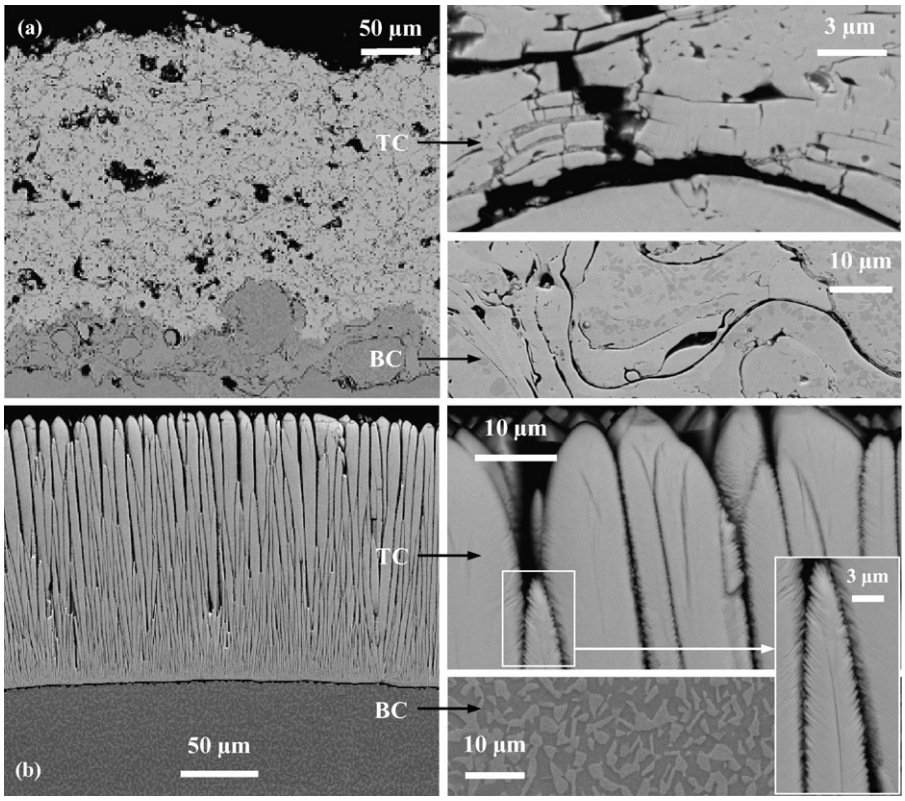

Fig. 5. (a) Backscattered electron (BSE) image of the microstructure of an air plasma sprayed YSZ TBC. As may be seen, both the bondcoat (BC) and topcoat (TC) have a lot of cavities and internal free surfaces created during the processing of the TBC. (b) BSE image of the microstructure of an electron beam-physical vapour deposited YSZ TBC. The BC is dense, and the TC shows the characteristic 'columnar' structure of EB-PVD TBCs, where each one of the columns has a 'feather-like' appearance.

and this corroborates the hypothesis that increasing levels of vibration in the PS coated beams increase the number of microcracks in the ceramic, resulting in higher levels of damping. The fact that the damping in APS coatings reaches a peak and then decreases above certain values of strain (vibration levels), is common for decays at all starting vibration levels and is a further evidence of the frictional nature of the damping mechanism of APS coatings.[14]

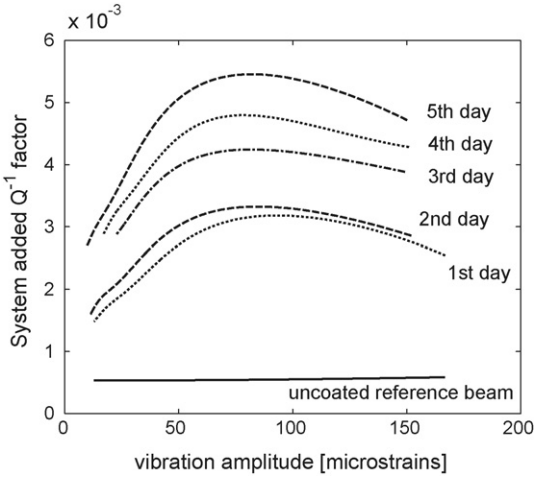

Fig. 6. Damping obtained for first level of strain in the different sessions of testing.

4. Conclusions

In this paper the non-linear mechanical behaviour of ceramic coating has been investigated. Different ceramic coatings have been taken in consideration, namely APS and EB-PVD deposited. The mechanical behaviour of the APS coating has been studied in greater detail, highlighting its different non-linearities. The results show that EB-PVD coatings possess higher Young's moduli than the APS coating (up to 77% higher), while APS shows five times higher damping, and these results have been correlated to their very different microstructures by means of SEM images. APS coatings have a dependence on the strain amplitude history. Further tests are planned at higher strain levels and at elevated temperatures, in order to study the mechanical properties as a function of temperature. Further SEM work is planned for analysing the nature of damage in the coatings responsible for the strain history dependence, and further tests will be run in order to investigate the strain history dependence of PVD coatings.

Acknowledgments

Work was supported in part by the European Community's Human Potential Programme under contract HPRN-CT-2002-00203 [SICMAC].[16] The authors acknowledge the financial support provided through the European Community's Human Potential Programme under contract HPRN-CT-2002-00203

[SICMAC]. The authors are grateful to Plasma & Thermal Coating Ltd., Newport, UK, for preparing all the APS coatings and to Mr. David Webster for assistance with the ADD test rig equipment.

References

1. Pawlowski, L., *The Science and Engineering of Thermal Spray Coatings*. John Wiley & Sons Ltd., England, UK, 1995.
2. Cao, X. Q., Vassen, R. and Stoever, D., Ceramic materials for thermal barrier coatings. *J. Eur. Ceram. Soc.*, 2004, **24**, 1–10.
3. Tassini, N., Lambrinou, K., Mircea, I., Patsias, S., Van der Biest, O. and Stanway, R., Comparison of the damping and stiffness properties of 8%Y.S. Zirconia ceramic coating deposited by APS and EB-PVD methods, *Proceedings SPIE 5760, Smart Structures and Materials, Damping and Isolation*, San Diego, California, In K.-W. Wang ed., 2005, pp. 109–117.
4. Patsias, S., Tassini, N. and Stanway, R., Hard ceramic coatings: an experimental study on a novel damping treatment, *Proceedings SPIE 5386, Smart Structures and Materials, Damping and Isolation*, San Diego, California, In K.-W. Wang ed., 2004, pp. 174–184.
5. Patsias, S. and Williams, R., Hard damping coatings: material properties and F.E. prediction method invited paper. In *Proceedings of 8th National Turbine Engine High Cycle Fatigue (HCF) Conference*, 2003.
6. Patsias, S., Tomlinson, G. R. and Jones, A. M., Initial studies into hard coatings for fan blade damping. In *Proceedings of 6th National Turbine Engine High Cycle Fatigue (HCF) Conference*, 2001.
7. Cross, K. R., Lull, W. R., Newman, R. L. and Cavanagh, J. R., Potential of graded coatings in vibration damping. *J. Aircraft*, 1973, **10**, 689–691.
8. Kroupa, F. and Plesek, J., Nonlinear elastic behaviour in compression of thermally sprayed materials. *Mater. Sci. Eng.*, 2002, **A328**, 1–7.
9. Rao, S. S., *Mechanical Vibrations*. Pearson Education Inc., New Jersey, 2004, pp. 141–146.
10. Nashif, A. D., Jones, D. I. G. and Henderson, J. P., *Vibration Damping*. John Wiley & Sons, New York, 1985, pp. 168–169.
11. Chang, G. C., Phucharoen, W. and Miller, R. A., Finite element thermal stress solutions for thermal barrier coatings. *Surf. Coat. Technol.*, 1987, **32**, 307–325.
12. Karlsson, A. M., Xu, T. and Evans, A. G., The effect of thermal barrier coating on the displacement instability in thermal barrier systems. *Acta Mater.*, 2002, **50**, 1211–1218.
13. *ABAQUS Standard User's Manual*, Version 6.3, Hibbit, Karlsson & Sorensen Inc., 2002.
14. Green, J. and Patsias, S., A preliminary approach for the modelling of a hard damping coating using friction elements. In *Proceedings of 7th National Turbine Engine High Cycle Fatigue (HCF) Conference*, 2002.
15. Van Den Abeele, K. and De Visscher, J., Damage assessment in reinforced concrete using spectral and temporal nonlinear vibration techniques. *Cem. Concr. Res.*, 2000, **30**, 1453–1464.
16. Internet Website, http://www.sicmac.net/.